Triangular Formation Maneuver Using Designed Mismatched Angles

Chen, Liangming; Cao, Ming; Garcia de Marina, Hector; Guo, Yanning; Kapitaniuk, Yuri

Published in:
Proceedings of the European Control Conference 2019

DOI:
10.23919/ECC.2019.8795944

2019 18th European Control Conference (ECC)
Napoli, Italy, June 25-28, 2019

Triangular formation maneuver using designed mismatched angles

Liangming Chen[1,2], Ming Cao[1], Hector Garcia de Marina[3], Yanning Guo[2], and Yuri Kapitanyuk[1]

Abstract— **This paper investigates the problem of triangular formation maneuver control for mobile 3-agent systems with bearing measurements. Different from controlling rigid formations' maneuvering by introducing a pair of mismatches per distance constraint, we introduce a pair of designed-mismatches per angle constraint which leads to the desired triangular formation shape. Considering that for the control of triangular formations with angle constraints, each agent aims at maintaining its own interior angle, to realize the formation maneuver control we design the mismatches into each agent's own desired interior angle. Two types of designed-mismatch are investigated: time-varying case and constant case. For the time-varying case, under the assumption that each agent can additionally measure the relative position from itself to the formation centroid, the triangular formation maneuver control algorithm is designed such that the desired maneuvering in terms of translation, rotation, and scaling can be realized. For the constant case, under the constraint that the desired triangular shape is known only once for the mismatch design, the triangular formation maneuver control algorithm is also proposed, and the angle dynamics are derived by using the dot product of two bearing vectors. Finally, simulation examples demonstrate the effectiveness of the theoretical results.**

I. INTRODUCTION

Multi-agent formations have attracted attention recently for the broad applications in, e.g., search and rescue of unmanned aerial vehicles [1], coordination of multiple mobile manipulators [2], and satellite formation flying for earth observation [3]. Two types of problems have been mainly investigated in the research community of multi-agent formation control, i.e., formation shape control and formation maneuver control [4], [5]. The works in [6]–[8] realized the control of desired formation shape described using inter-agent displacements, distances, and bearings respectively. However, in many practical applications, formations are expected to be "maneuverable", i.e., capable of translating, scaling, and rotating to adapt to the complicated environment in practice [6]. For example, when a group of flying unmanned aerial vehicles aims at smoothly passing through some areas containing buildings or other types of obstacles, they need to alter their motion speed, direction, and even size of the whole formation. Therefore, some researchers started studying the formation maneuver control which requires the achievement of not only the desired geometric formation shape, but also the formation as a whole being capable of translating, scaling, rotating or moving in combination of such maneuvering as dictated by the desired formation [9].

To solve the formation maneuver control problem, some researchers have proposed different approaches towards different types of formation shape description and available information. For the formation shape described by displacements, the work in [3] realized the translational formation maneuver control with the measurements of relative positions. For rigid formations with distance constraints, the formation maneuver control algorithm was designed in [10] by introducing a pair of mismatches per distance constraint, in which the rotational and translational maneuvering was realized under the measurement of local relative positions. For the formation shape described by inter-agent bearings, the work in [9] realized the translational and scaling formation maneuver control with the measurement of relative positions. Note that these works [3], [9], [10] cannot fully realize the formation maneuvering of scaling, rotation, and translation at the same time. To realize the formation maneuver control with the capacity of translation, rotation and scaling, some other approaches or tools were proposed, including leader-follower affine formation [11], barycentric coordinate-based approach [12], and complex Laplacian-based approach [13]. However, for most of the proposed formation maneuver control algorithms [3], [9]–[13], the measurements of relative position are required. Compared with relative position measurements, bearing measurements are becoming cheaper, more reliable and accessible. With the rapid development of sensor technologies, bearing can be measured using the locally equipped passive radar, passive sonar, and vision-based camera [14].

Therefore, motivated by the existing results, this study aims at realizing the formation maneuver control with the capacity of translation, rotation and scaling under bearing measurements. As the start for this challenging problem, we first focus on the case of three agents and triangular formation in this paper. To solve this problem, we employ the mismatch-based approach which was investigated in [10], [15], but modify it as 'designed-mismatch' in this paper since the mismatch is added into each agent's own desired interior angle which is different from the mismatch used in the existing maneuver control of rigid formations. Two types of designed-mismatch are investigated: time-varying case and constant case respectively. For the time-varying case, under the assumption that each agent can additionally measure the relative position from itself to the formation centroid, the triangular formation maneuver control algorithm is designed

[1]L. Chen, M. Cao, and Y. Kapitanyuk are with Faculty of Science and Engineering, University of Groningen, Groningen, 9747 AG, The Netherlands. l.m.chen@rug.nl, m.cao@rug.nl, yura.kapitanyuk@gmail.com

[2]L. Chen and Y. Guo are with Department of Control Science and Engineering, Harbin Institute of Technology, Harbin, 150001, China. guoyn@hit.edu.cn

[3]H. G. Marina is with Unmanned Aerial Systems Center, Maersk Mc-Kinney Moller Institute, Southern University of Denmark, Denmark. hgm@mmmi.sdu.dk

such that the steady-state formation can move with translation, rotation, and scaling. For the constant case, under the constraint that the desired triangular shape is known for the mismatch design, the triangular formation maneuver control algorithm is proposed with only bearing measurements.

The contributions of this study can be summarized as follows. The formation maneuver control is realized with translation, rotation, and scaling at the same time under the bearing measurements. Compared with other formation maneuver control approaches [3], [9], [10], more motion freedoms are realized in this study. For the constant designed-mismatch case, the formation maneuver control algorithm only needs the bearing measurements, without requiring the measurements of relative positions [3], [9]–[13]. The angle dynamics are derived by using the dot product of two bearing vectors, which are different from the papers e.g. [16].

The rest of this paper is organized as follows. Section II introduces basic background knowledge and problem formulation. In Section III, we give the main results, including the time-varying mismatch case and constant mismatch case. In Section IV, the theoretical results are illustrated by numerical simulations. The conclusions are given in Section V.

II. Preliminaries and Problem Formulation

For triangular formation with three agents, we first define the agents' dynamics and the bearing measurements. Then, the research problem is formally formulated.

A. Agents' dynamics

For a 3-agent system moving in the plane, the motion dynamics of an agent i are governed by [16]

$$\dot{p}_i = u_i = v_i \begin{bmatrix} \cos\beta_i \\ \sin\beta_i \end{bmatrix}, i = 1,2,3 \tag{1}$$

where $p_i = [x_i, y_i]^T \in \mathbb{R}^2$ denotes the position of agent i, and $v_i \in \mathbb{R}$ is the moving speed, and the heading angle β_i is defined counter-clockwise with respect to agent i's local x-direction and always takes its value from $[0, 2\pi)$. Both v_i and β_i are the control inputs to be determined.

B. Bearing measurements

Agent i measures the bearing $\phi_{ij} \in [0, 2\pi), \forall j \in \mathcal{N}_i$ towards agent j evaluated counter-clockwise from its local x_i-direction, and here $\mathcal{N}_i$ denotes the set of the neighbours of agent i. For triangular formation, $\mathcal{N}_i = \{(i+1) \bmod 3, (i-1) \bmod 3\} \in \{1,2,3\}$, and $\phi_{i(i+1)} = \phi_{31}$ when $i = 3$, $\phi_{i(i-1)} = \phi_{13}$ when $i = 1$.

First, we introduce the auxiliary angle

$$\theta_i = |\phi_{i(i+1)} - \phi_{i(i-1)}| \in [0, 2\pi) \tag{2}$$

which is the angle measured counter-clockwise from $\min\{\phi_{i(i+1)}, \phi_{i(i-1)}\}$ to $\max\{\phi_{i(i+1)}, \phi_{i(i-1)}\}$ with respect to agent i's local x-direction.

Then, we define the interior angle α_i to be

$$\alpha_i = \begin{cases} \theta_i, & \text{if } \theta_i \le \pi \\ 2\pi - \theta_i, & \text{otherwise} \end{cases} \tag{3}$$

where $\alpha_i \in [0, \pi]$ represents agent i's interior angle in the triangle $(i-1)i(i+1)$, see Fig.1.

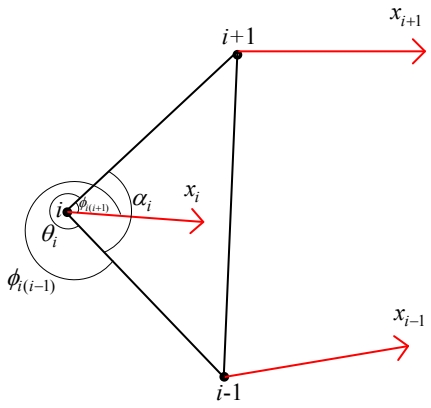

Fig. 1: The bearing measurements.

C. Problem formulation

The goal of this paper is to design formation maneuver control algorithm u_i for each agent $i, i = 1,2,3$ such that the closed-loop system can achieve:

(1) The desired triangular formation shape

$$\lim_{t\to\infty}(\alpha_i - \alpha_i^*) = 0, \forall i = 1,2,3 \tag{4}$$

where $\alpha_i^* \in (0, \pi)$ denotes agent i's desired interior angle, and naturally $\alpha_1^* + \alpha_2^* + \alpha_3^* = \pi$.

(2) Translational formation maneuver

$$\lim_{t\to\infty} \dot{p}_i = \dot{p}_j = v_c^*, \forall i, j = 1,2,3 \tag{5}$$

where $v_c^* \in \mathbb{R}^2$ is the steady-state translational velocity.

(3) Rotational formation maneuver

$$\lim_{t\to\infty}(\dot{p}_i \cdot p_i^b) = 0, \forall i = 1,2,3 \tag{6}$$

$$\lim_{t\to\infty} \frac{v_i}{\|p_i^b\|} = \lim_{t\to\infty} \frac{v_j}{\|p_j^b\|} = \omega^*, \forall i, j = 1,2,3 \tag{7}$$

where $\cdot$ represents the dot product of two vectors, $p_i^b = p_i - p_c = p_i - \frac{p_i + p_{i+1} + p_{i-1}}{3}$ denotes the vector from the formation centroid p_c to agent i's position p_i, $\omega^* \in \mathbb{R}$ is the steady-state rotational angular velocity.

(4) Scaling formation maneuver

$$\lim_{t\to\infty} \dot{p}_i = s(t) \lim_{t\to\infty} p_i^b = v_{si}^* \lim_{t\to\infty} \frac{p_i^b}{\|p_i^b\|}, \forall i = 1,2,3 \tag{8}$$

where $v_{si}^* \in \mathbb{R}$ is agent i's steady-state scaling velocity, and $s(t) \in \mathbb{R}^+$ is a time-varying positive real number which implies that $\dot{p}_i/\|\dot{p}_i\| = p_i^b/\|p_i^b\|$ and $\|\dot{p}_i\|/\|p_i^b\| = \|\dot{p}_j\|/\|p_j^b\| = s(t), \forall i, j = 1,2,3$ as $t \to \infty$.

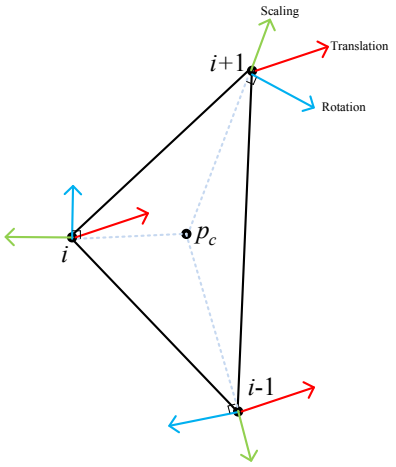

Fig. 2: Formation maneuver: translation, rotation and scaling.

III. Main Results

In this section, we aim at solving the triangular formation maneuver control problem. First, we will introduce a modified bearing formation control algorithm with a pair of designed-mismatches per angle constraint. Then, for the cases of time-varying and constant designed-mismatches, the formation maneuver control algorithms and the corresponding stability analysis will be given respectively.

A. Modified bearing formation control algorithm

In [16], by using the local bearing measurements, three agents achieved a triangular formation shape described by three interior angles $\alpha_i^*, i = 1, 2, 3$. The control algorithms designed in [16] are

$$v_i = -k_i(\alpha_i - \alpha_i^*), i = 1, 2, 3 \tag{9}$$

$$\beta_i = \begin{cases} \alpha_i/2 + \min\{\phi_{i(i+1)}, \phi_{i(i-1)}\}, & \text{if } \theta_i \le \pi \\ \alpha_i/2 + \max\{\phi_{i(i+1)}, \phi_{i(i-1)}\}, & \text{if } \theta_i > \pi \end{cases} \tag{10}$$

which physically means that agent i always moves towards the bisection of the interior angle α_i with the speed $|k_i(\alpha_i - \alpha_i^*)|$, where k_i is a positive constant.

Actually, when the three agents are not collinear, the control algorithms (9)-(10) can be equivalently written as

$$u_i = -k_i(\alpha_i - \alpha_i^*)\frac{z_{i(i+1)} + z_{i(i-1)}}{\|z_{i(i+1)} + z_{i(i-1)}\|} \tag{11}$$

where the unit vector $z_{i(i+1)} = \frac{p_{i+1} - p_i}{\|p_{i+1} - p_i\|} = \begin{bmatrix} \cos\phi_{i(i+1)} \\ \sin\phi_{i(i+1)} \end{bmatrix}$ is a function of bearing $\phi_{i(i+1)}$. Since $\|z_{i(i+1)} + z_{i(i-1)}\| > 0$, we propose another simple control algorithm

$$\begin{aligned} u_i =& -k_i(\alpha_i - \alpha_i^*)(z_{i(i+1)} + z_{i(i-1)}) \\ =& -k_i(\alpha_i - \alpha_i^*)z_{i(i+1)} - k_i(\alpha_i - \alpha_i^*)z_{i(i-1)} \end{aligned} \tag{12}$$

Now, we introduce a pair of designed-mismatches per angle constraint α_i^* into (12) such that the formation maneuvering with translation, rotation, and scaling can be realized. By following the method given in [10], we modify the formation control algorithm as

$$\begin{aligned} u_i =& -k_i(\alpha_i - \alpha_i^* - \frac{\mu_i}{k_i})z_{i(i+1)} - k_i(\alpha_i - \alpha_i^* - \frac{\tilde{\mu}_i}{k_i})z_{i(i-1)} \\ =& -k_i(\alpha_i - \alpha_i^*)(z_{i(i+1)} + z_{i(i-1)}) \\ &+ \mu_i z_{i(i+1)} + \tilde{\mu}_i z_{i(i-1)} \end{aligned} \tag{13}$$

where $\mu_i \in \mathbb{R}$ and $\tilde{\mu}_i \in \mathbb{R}$ are the designed-mismatches associated with agent i's desired angle α_i^*. Note that the triangular shape described by interior angles has the invariance of translation, rotation, and scaling. Thus, we can use $-k_i(\alpha_i - \alpha_i^*)(z_{i(i+1)} + z_{i(i-1)})$ to realize the desired triangular shape, and $\mu_i z_{i(i+1)} + \tilde{\mu}_i z_{i(i-1)}$ to realize the desired maneuvering in terms of translation, rotation, and scaling. The steady-state velocity of each agent $\dot{p}_i^*$ at the desired triangular formation shape can be decomposed into

$$\begin{aligned} \dot{p}_i^* =& \dot{p}_{i(translation)}^* + \dot{p}_{i(rotation)}^* + \dot{p}_{i(scaling)}^* \\ =& v_c^* + \omega^* E p_i^b + v_{si}^* \frac{p_i^b}{\|p_i^b\|} = \mu_i z_{i(i+1)} + \tilde{\mu}_i z_{i(i-1)} \end{aligned} \tag{14}$$

where $E = \begin{bmatrix} 0 & -1 \\ 1 & 0 \end{bmatrix}$ is a skew-symmetric matrix, and Ep_i^b represents turning vector p_i^b with $\pi/2$ along counter-clockwise direction. Note that in (14), $z_{i(i+1)}$ is the information related to bearing measurement $\phi_{i(i+1)}$, but p_i^b is the vector from the formation centroid p_c to agent i's position p_i which should be additionally measured. Therefore, in the following, we design time-varying designed-mismatches when both $z_{ij}, j \in \mathcal{N}_i$ and p_i^b can be measured, and constant designed-mismatches when only z_{ij} can be measured.

B. Time-varying designed-mismatches

Now, we use the time-varying designed-mismatches to realize the desired maneuvering under the measurements of z_{ij} and p_i^b. In the following, we first illustrate how to design $\mu_i(t)$ and $\tilde{\mu}_i(t)$, then analyze the closed-loop stability.

1) Translation: According to (14), one has

$$v_c^* = \mu_1(t)z_{12} + \tilde{\mu}_1(t)z_{13} \tag{15}$$

$$v_c^* = \mu_2(t)z_{23} + \tilde{\mu}_2(t)z_{21} \tag{16}$$

$$v_c^* = \mu_3(t)z_{31} + \tilde{\mu}_3(t)z_{32} \tag{17}$$

where we consider that the three agents are not collinear. Then, $\mu_i(t), \tilde{\mu}_i(t), i = 1, 2, 3$ can be calculated by

$$\begin{bmatrix} \mu_i(t) \\ \tilde{\mu}_i(t) \end{bmatrix} = \begin{bmatrix} z_{i(i+1)}(1) & z_{i(i-1)}(1) \\ z_{i(i+1)}(2) & z_{i(i-1)}(2) \end{bmatrix}^{-1} \begin{bmatrix} v_c^*(1) \\ v_c^*(2) \end{bmatrix} \tag{18}$$

where $z_{i(i+1)}(1)$ and $z_{i(i+1)}(2)$ denote the first and second elements of vector $z_{i(i+1)}$. Note that (15)-(17) are equivalent to adding the same v_c^* to all agents.

2) Rotation: According to (14), one has

$$\omega^* E p_1^b = \mu_1(t)z_{12} + \tilde{\mu}_1(t)z_{13} \tag{19}$$

$$\omega^* E p_2^b = \mu_2(t)z_{23} + \tilde{\mu}_2(t)z_{21} \tag{20}$$

$$\omega^* E p_3^b = \mu_3(t)z_{31} + \tilde{\mu}_3(t)z_{32} \tag{21}$$

By using a similar way as given in (15)-(18), $\mu_i(t), \tilde{\mu}_i(t), i = 1, 2, 3$ can be calculated.

3) Scaling: According to (14) and (8), one has

$$s(t)p_1^b = \mu_1(t)z_{12} + \tilde{\mu}_1(t)z_{13} \tag{22}$$

$$s(t)p_2^b = \mu_2(t)z_{23} + \tilde{\mu}_2(t)z_{21} \tag{23}$$

$$s(t)p_3^b = \mu_3(t)z_{31} + \tilde{\mu}_3(t)z_{32} \tag{24}$$

Then, $\mu_i(t), \tilde{\mu}_i(t), i = 1, 2, 3$ can be calculated.

Now, we give our main result.

Theorem 1: For a 3-agent formation system described by (1), with the formation control algorithm (13) and time-varying mismatches $\mu_i(t), \tilde{\mu}_i(t), i = 1, 2, 3$ designed in (15)-(17), (19)-(21), and (22)-(24), if the initial angle error $e_i(0)$ and the designed-mismatches are sufficiently small and $\alpha_i(0) \neq 0$, the 3-agent formation asymptotically converges to its desired shape and maneuvers with prescribed translation, rotation, and scaling, respectively.

Proof: Note that the angle dynamics are influenced by the combination of formation shape control part $-k_i(\alpha_i - \alpha_i^*)(z_{i(i+1)} + z_{i(i-1)})$ and maneuver control part $\mu_i z_{i(i+1)} + \tilde{\mu}_i z_{i(i-1)}$. By following the same analysis steps given in [16], one has that when we only consider the formation shape control part, the angle dynamics can be described as

$$\dot{e} = \begin{bmatrix} \dot{\alpha}_1 \\ \dot{\alpha}_2 \\ \dot{\alpha}_3 \end{bmatrix} = F(e)e = \begin{bmatrix} -g_1 & f_{12} & f_{13} \\ f_{21} & -g_2 & f_{23} \\ f_{31} & f_{32} & -g_3 \end{bmatrix} \begin{bmatrix} \alpha_1 - \alpha_1^* \\ \alpha_2 - \alpha_2^* \\ \alpha_3 - \alpha_3^* \end{bmatrix} \tag{25}$$

where $e_i = \alpha_i - \alpha_i^*$, $f_{i(i+1)} = \frac{k_{i+1}}{l_{i(i+1)}}||z_{(i+1)i} + z_{(i+1)(i-1)}|| \sin\frac{\alpha_{i+1}}{2}$, $g_i = (\frac{k_i}{l_{i(i+1)}} + \frac{k_i}{l_{i(i-1)}})||z_{i(i+1)} + z_{i(i-1)}|| \sin\frac{\alpha_i}{2}, i = 1, 2, 3$, where l_{ij} denotes the distance between agents i and j. Following the local analysis method examing eigenvalues of the linearized system [16], one can easily obtain the local stability of (25).

When we only consider the maneuver control part, the angle dynamics can be described by $\dot{e} = 0$ since time-varying designed-mismatches $\mu_i(t), \tilde{\mu}_i(t), i = 1, 2, 3$ designed in (15)-(17), (19)-(21), and (22)-(24) have no contribution to the angle changes $\dot{\alpha}_i$.

Combining the above two parts, one can get the local stability of the closed-loop system (25), i.e., $\lim_{t\to\infty}(\alpha_i - \alpha_i^*) = 0, \forall i = 1, 2, 3$. Since $\dot{e}_i = -g_i(\alpha_i - \alpha_i^*) + f_{i(i+1)}(\alpha_{i+1} - \alpha_{i+1}^*) + f_{i(i-1)}(\alpha_{i-1} - \alpha_{i-1}^*)$, when $\alpha_i \to \pi$, one has $\dot{e}_i < 0$, which implies the three agents will not become collinear if they are not initially collinear at the initial time. Thus, p_i^b and (18) are well-defined. Then, according to (1) and (13), one has $\lim_{t\to\infty} \dot{p}_i = \mu_i z_{i(i+1)} + \tilde{\mu}_i z_{i(i-1)}$. By using (15)-(17), (19)-(21), and (22)-(24), one has that the maneuvering defined in (5)-(8) is achieved. ■

C. Constant designed-mismatches

Now, we consider that agent i can only measure $z_{i(i+1)}$ and $z_{i(i-1)}$, and the designed-mismatches μ_i and $\tilde{\mu}_i$ are constant. To achieve the maneuvering of translation, rotation and scaling, we require that the steady-state formation geometric shape is known for the design of mismatches. By following the similar steps given in Sections A and B, we give the following design procedure for the constant designed-mismatch case.

1) Translation: According to (14), one has

$$v_c^* = \mu_1 z_{12}^* + \tilde{\mu}_1 z_{13}^* \tag{26}$$

$$v_c^* = \mu_2 z_{23}^* + \tilde{\mu}_2 z_{21}^* \tag{27}$$

$$v_c^* = \mu_3 z_{31}^* + \tilde{\mu}_3 z_{32}^* \tag{28}$$

where $z_{i(i+1)}^*$ is the unit vector corresponding to the steady-state formation geometric shape. Then, $\mu_i, \tilde{\mu}_i, i = 1, 2, 3$ can be calculated by

$$\begin{bmatrix} \mu_i \\ \tilde{\mu}_i \end{bmatrix} = \begin{bmatrix} z_{i(i+1)}^*(1) & z_{i(i-1)}^*(1) \\ z_{i(i+1)}^*(2) & z_{i(i-1)}^*(2) \end{bmatrix}^{-1} \begin{bmatrix} v_c^*(1) \\ v_c^*(2) \end{bmatrix} \tag{29}$$

2) Rotation: According to (14), one has

$$\omega^* E(p_1^b)^* = \mu_1 z_{12}^* + \tilde{\mu}_1 z_{13}^* \tag{30}$$

$$\omega^* E(p_2^b)^* = \mu_2 z_{23}^* + \tilde{\mu}_2 z_{21}^* \tag{31}$$

$$\omega^* E(p_3^b)^* = \mu_3 z_{31}^* + \tilde{\mu}_3 z_{32}^* \tag{32}$$

where $(p_i^b)^* = p_i^* - p_c^* = \frac{(p_i - p_{i+1})^* + (p_i - p_{i-1})^*}{3}$. Then, $\mu_i, \tilde{\mu}_i, i = 1, 2, 3$ can be calculated.

3) Scaling: According to (14), one has

$$v_{s1}^* \frac{(p_1^b)^*}{\|(p_1^b)^*\|} = k_s(p_1^b)^* = \mu_1 z_{12}^* + \tilde{\mu}_1 z_{13}^* \tag{33}$$

$$v_{s2}^* \frac{(p_2^b)^*}{\|(p_2^b)^*\|} = k_s(p_2^b)^* = \mu_2 z_{23}^* + \tilde{\mu}_2 z_{21}^* \tag{34}$$

$$v_{s3}^* \frac{(p_3^b)^*}{\|(p_3^b)^*\|} = k_s(p_3^b)^* = \mu_3 z_{31}^* + \tilde{\mu}_3 z_{32}^* \tag{35}$$

where $v_{si}^*/\|(p_i^b)^*\| = v_{sj}^*/\|(p_j^b)^*\| = k_s > 0$. Then, $\mu_i, \tilde{\mu}_i, i = 1, 2, 3$ can be calculated.

Now, we give our main result.

Theorem 2: For a 3-agent formation system described by (1), with the formation control algorithm (13) and constant mismatches $\mu_i, \tilde{\mu}_i, i = 1, 2, 3$ designed in (26)-(28), (30)-(32), and (33)-(35), if the initial angle error $e_i(0)$ and the designed-mismatches are sufficiently small and $\alpha_i(0) \neq 0$, the 3-agent formation asymptotically converges to its desired shape and maneuvers with prescribed translation, rotation, and scaling, respectively.

Proof: To analyze the convergence of e_i, we first aim at obtaining the dynamics of the interior angles $\alpha_i, i = 1, 2, 3$. Note that the analysis method given in [16] cannot be used in this case because of the existence of $\mu_i z_{i(i+1)} + \tilde{\mu}_i z_{i(i-1)}$. Instead, the angle dynamics can be obtained by using the dot product of two bearings, from which one has the following angle dynamics

$$\begin{aligned} \dot{e} &= [\dot{\alpha}_1 \ \ \dot{\alpha}_2 \ \ \dot{\alpha}_3]^T = F(e)e + H(e) \\ &= \begin{bmatrix} -g_1 & f_{12} & f_{13} \\ f_{21} & -g_2 & f_{23} \\ f_{31} & f_{32} & -g_3 \end{bmatrix} \begin{bmatrix} \alpha_1 - \alpha_1^* \\ \alpha_2 - \alpha_2^* \\ \alpha_3 - \alpha_3^* \end{bmatrix} + \begin{bmatrix} h_1 \\ h_2 \\ h_3 \end{bmatrix} \end{aligned} \tag{36}$$

where

$$g_i = \sin\alpha_i(k_i/l_{i(i+1)} + k_i/l_{i(i-1)}),$$

$$f_{ij} = k_j(\sin\alpha_j)/l_{ij},$$

$$h_i = \frac{\tilde{\mu}_i \sin\alpha_i - \mu_{i+1}\sin\alpha_{i+1}}{l_{i(i+1)}} + \frac{\mu_i \sin\alpha_i - \tilde{\mu}_{i-1}\sin\alpha_{i-1}}{l_{i(i-1)}}.$$

To analyze the local stability of (36), we employ the stability analysis method given in [16]. Since $e_1+e_2+e_3=0$, one has the following sub-dynamics

$$\begin{aligned}\dot{e}_s &= \begin{bmatrix}\dot{\alpha}_1\\ \dot{\alpha}_2\end{bmatrix} = F_s(e_s)e_s + H_s(e_s) \qquad (37)\\ &= \begin{bmatrix}-(g_1+f_{13}) & f_{12}-f_{13}\\ f_{21}-f_{23} & -(g_2+f_{23})\end{bmatrix}\begin{bmatrix}e_1\\ e_2\end{bmatrix} + \begin{bmatrix}h_1(\alpha_1,\alpha_2)\\ h_2(\alpha_1,\alpha_2)\end{bmatrix}\end{aligned}$$

where $h_1(\alpha_1,\alpha_2) = \frac{\tilde{\mu}_1\sin\alpha_1-\mu_2\sin\alpha_2}{l_{12}} + \frac{\mu_1\sin\alpha_1-\tilde{\mu}_3\sin(\alpha_1+\alpha_2)}{l_{13}}$, $h_2(\alpha_1,\alpha_2) = \frac{\mu_2\sin\alpha_2-\tilde{\mu}_1\sin\alpha_1}{l_{21}} + \frac{\tilde{\mu}_2\sin\alpha_2-\mu_3\sin(\alpha_1+\alpha_2)}{l_{23}}$.

The linearized system of (37) around the origin can be written as

$$\dot{\epsilon}_s = A\epsilon_s + B\epsilon_s = (A+B)\epsilon_s \qquad (38)$$

where $A = F_s(\epsilon_s)$, and $B = \frac{\partial H_s}{\partial e_s}|_{e_s=0}$.

According to [16], it can be easily verified that

$$\mathrm{tr}(F_s(\epsilon_s))|_{\epsilon_s=0} < 0 \qquad (39)$$

$$\det(F_s(\epsilon_s))|_{\epsilon_s=0} > 0 \qquad (40)$$

which imply that all the eigenvalues of $F_s(\epsilon_s)|_{\epsilon_s=0}$ have negative real parts. Therefore $A = F_s(\epsilon_s)|_{\epsilon_s=0}$ is a Hurwitz matrix. Then, according to the Lyapunov theorem [17], there always exists a constant positive definite matrix P such that $Q = -(PA + A^TP)$ is negative definite.

Consider the following Lyapunov function candidate

$$V = \epsilon_s^T P \epsilon_s \qquad (41)$$

Taking the time-derivative of (41) gives

$$\begin{aligned}\dot{V} &\le -\lambda_{\min}(Q)||\epsilon_s||^2 + \epsilon_s^T(B^TP + PB)\epsilon_s\\ &\le (-\lambda_{\min}(Q) + q)||\epsilon_s||^2 \qquad (42)\end{aligned}$$

where $q = \lambda_{\max}(B^TP + PB)$. For a neighborhood of the equilibrium $\alpha_i = \alpha_i^*$, one can have $\lambda_{\min}(Q) \ge q$ by choosing small designed-mismatches $\mu_i, \tilde{\mu}_i$ since q grows with μ continuously and $q(\mu) \ge q(0) = 0$, or big k_i which only makes $\lambda_{\min}(Q)$ bigger but not $\lambda_{\max}(B^TP+PB)$. Since P can be calculated for given Q and A according to [17, Theorem 4.6], the stability for given $\mu_i, \tilde{\mu}_i$ can be known.

When $\lambda_{\min}(Q) \ge q$, $(A+B)$ is Hurwitz and the sub-dynamics (37) are locally asymptotically stable. Since $e_1 = e_2 = 0$ implies $e_3 = 0$, the overall dynamic system (36) is locally stable. Note that $\mu_i, \tilde{\mu}_i, i = 1,2,3$ are designed according to the steady-state geometric shape, it can be obtained that when z_{ij}^* and $(p_i^b)^*$ describing the steady-state geometric shape is sufficiently close to the steady-state formation, the final formation will maneuver with translation, rotation and scaling. ■

Remark 1: Note that for the time-varying designed-mismatch case, to avoid using the information of desired geometric shape and realizing distributively the calculation of $\mu_i(t), \tilde{\mu}_i(t), i = 1,2,3$ in (22)-(24), one can choose the first equality in (8) and set $s(t) = 1$, which will result in an uncontrolled scaling velocity. For the constant designed-mismatch case, since the geometric triangular shape is known for the designed-mismatch design, the scaling velocity can be adjusted by choosing different k_s in (33)-(35).

IV. Simulation Examples

In this section, we present numerical simulation examples to verify the effectiveness of the proposed formation maneuver control algorithms. For all the cases, the desired angles are set as $\alpha_i^* = \pi/3, i = 1,2,3$.

(1) Time-varying mismatch case

The following figures show the maneuvering of translation, rotation and scaling respectively.

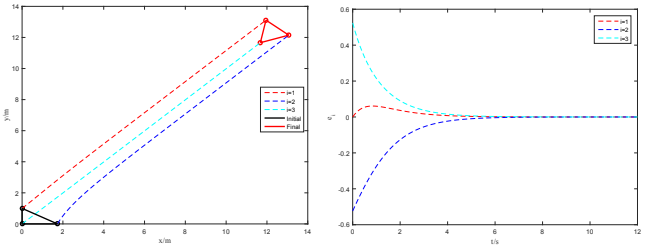

(a) Formation trajectories (b) Relative angle errors

Fig. 3: Translational maneuver

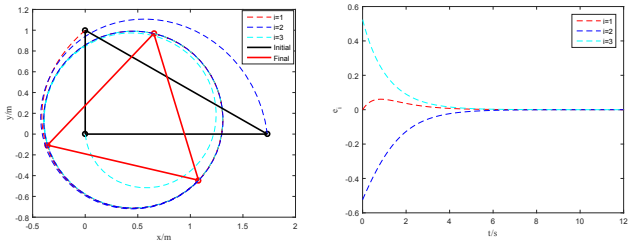

(a) Formation trajectories (b) Relative angle errors

Fig. 4: Rotational maneuver

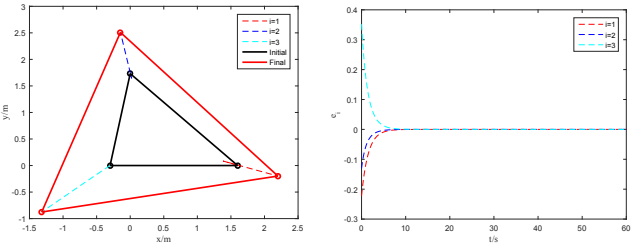

(a) Formation trajectories (b) Relative angle errors

Fig. 5: Scaling maneuver

(2) Constant mismatch case

The following figures show the maneuvering of translation, rotation and scaling respectively.

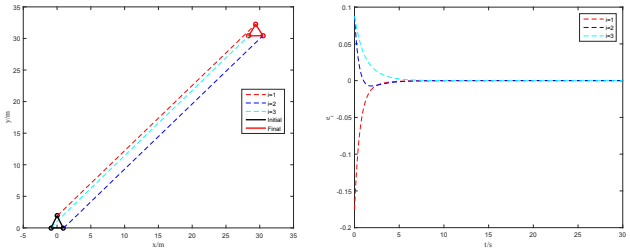

(a) Formation trajectories (b) Relative angle errors

Fig. 6: Translational maneuver

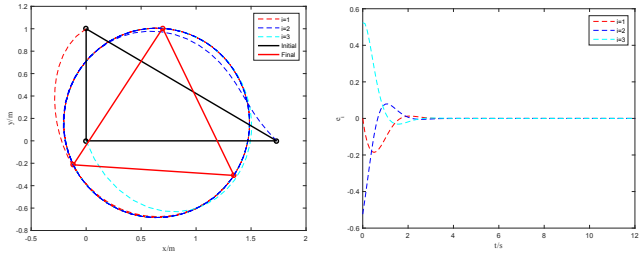

(a) Formation trajectories (b) Relative angle errors

Fig. 7: Rotational maneuver

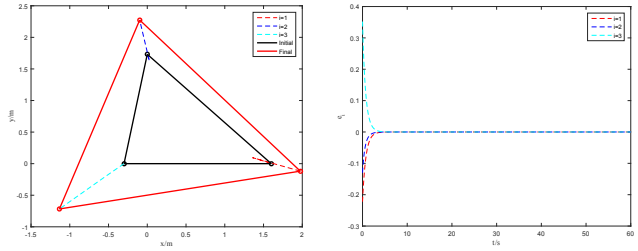

(a) Formation trajectories (b) Relative angle errors

Fig. 8: Scaling maneuver

According to Figs. 3-8, we can see that the desired triangular formation shape and the desired maneuvering are achieved under the proposed formation control algorithms. Note that in Figs. 3-8, the relative angle errors converge to zero, which illustrate the asymptotically stability of the proposed maneuver control algorithms.

V. CONCLUSIONS AND FUTURE WORKS

This study realizes the triangular formation maneuver control under bearing measurements by using a designed-mismatch angle approach. Two types of designed-mismatches are investigated: time-varying case and constant case. For both cases, the triangular formation maneuver control algorithms are proposed to realize the desired maneuvering. To analyze the stability of the constant designed-mismatch case, the angle dynamics are derived by using the dot product of two bearings. Finally, simulation examples demonstrate the effectiveness of the theoretic results.

Many studies about formation maneuver control focused on rigid formation shapes and arbitrary number of agents. It is very challenging to solve the general problem with angle rigid formation shapes and arbitrary number of agents. We are also interested in taking the proposed triangular formation maneuver control strategy to trajectory tracking or cooperative transportation tasks.

VI. ACKNOWLEDGMENTS

This work was supported by the National Natural Science Foundation of China (Grant No. 61876050, 61673135, 61603114). The work of L. Chen was supported by the China Scholarship Council.

REFERENCES

[1] B. D. Anderson, B. Fidan, C. Yu, and D. Walle, "UAV formation control: Theory and application," in *Recent Advances in Learning and Control*. Springer, 2008, pp. 15–33.

[2] H. Bai and J. T. Wen, "Cooperative load transport: A formation-control perspective," *IEEE Transactions on Robotics*, vol. 26, no. 4, pp. 742–750, 2010.

[3] L. Chen, Y. Guo, C. Li, and J. Huang, "Satellite formation-containment flying control with collision avoidance," *Journal of Aerospace Information Systems*, vol. 15, no. 5, pp. 253–270, 2018.

[4] B. D. Anderson, C. Yu, and J. M. Hendrickx, "Rigid graph control architectures for autonomous formations," *IEEE Control Systems Magazine*, vol. 28, no. 6, 2008.

[5] K. K. Oh, M. C. Park, and H. S. Ahn, "A survey of multi-agent formation control," *Automatica*, vol. 53, pp. 424–440, 2015.

[6] Q. Yang, M. Cao, H. G. de Marina, H. Fang, and J. Chen, "Distributed formation tracking using local coordinate systems," *Systems & Control Letters*, vol. 111, pp. 70–78, 2018.

[7] M. Cao, C. Yu, and B. D. Anderson, "Formation control using range-only measurements," *Automatica*, vol. 47, no. 4, pp. 776–781, 2011.

[8] S. Zhao and D. Zelazo, "Bearing rigidity and almost global bearing-only formation stabilization," *IEEE Transactions on Automatic Control*, vol. 61, no. 5, pp. 1255–1268, 2016.

[9] S. Zhao and D. Zelazo, "Translational and scaling formation maneuver control via a bearing-based approach," *IEEE Transactions on Control of Network Systems*, vol. 4, no. 3, pp. 429–438, 2017.

[10] H. G. de Marina, B. Jayawardhana, and M. Cao, "Distributed rotational and translational maneuvering of rigid formations and their applications," *IEEE Transactions on Robotics*, vol. 32, no. 3, pp. 684–697, 2016.

[11] S. Zhao, "Affine formation maneuver control of multi-agent systems," *IEEE Transactions on Automatic Control*, 2018.

[12] T. Han, Z. Lin, R. Zheng, and M. Fu, "A barycentric coordinate-based approach to formation control under directed and switching sensing graphs," *IEEE Transactions on Cybernetics*, vol. 48, no. 4, pp. 1202–1215, 2018.

[13] Z. Han, L. Wang, Z. Lin, and R. Zheng, "Formation control with size scaling via a complex laplacian-based approach." *IEEE Trans. Cybernetics*, vol. 46, no. 10, pp. 2348–2359, 2016.

[14] A. K. Das, R. Fierro, V. Kumar, J. P. Ostrowski, J. Spletzer, and C. J. Taylor, "A vision-based formation control framework," *IEEE Transactions on Robotics and Automation*, vol. 18, no. 5, pp. 813–825, 2002.

[15] H. G. De Marina, B. Jayawardhana, and M. Cao, "Taming mismatches in inter-agent distances for the formation-motion control of second-order agents," *IEEE Transactions on Automatic Control*, vol. 63, no. 2, pp. 449–462, 2018.

[16] M. Basiri, A. N. Bishop, and P. Jensfelt, "Distributed control of triangular formations with angle-only constraints," *Systems & Control Letters*, vol. 59, no. 2, pp. 147–154, 2010.

[17] H. K. Khalil, *Nonlinear systems, 3rd.* Upper Saddle River, NJ: Prentice Hall, 2002.